Pushing the Limits of 3D Shape Generation at Scale

Yu Wang[1,*] **Xuelin Qian**[1,*] **Jingyang Huo**[1] **Tiejun Huang**[2] **Bo Zhao**[2,†] **Yanwei Fu**[1,†]
[1]Fudan University [2]Beijing Academy of Artificial Intelligence
{yu_w13,xlqian,yanweifu}@fudan.edu.cn zhaobo@baai.ac.cn

Abstract

We present a significant breakthrough in 3D shape generation by scaling it to unprecedented dimensions. Through the adaptation of the Auto-Regressive model and the utilization of large language models, we have developed a remarkable model with an astounding 3.6 billion trainable parameters, establishing it as the largest 3D shape generation model to date, named *Argus-3D*. Our approach addresses the limitations of existing methods by enhancing the quality and diversity of generated 3D shapes. To tackle the challenges of high-resolution 3D shape generation, our model incorporates tri-plane features as latent representations, effectively reducing computational complexity. Additionally, we introduce a discrete codebook for efficient quantization of these representations. Leveraging the power of transformers, we enable multi-modal conditional generation, facilitating the production of diverse and visually impressive 3D shapes. To train our expansive model, we leverage an ensemble of publicly-available 3D datasets, consisting of a comprehensive collection of approximately 900,000 objects from renowned repositories such as ModelNet40, ShapeNet, Pix3D, 3D-Future, and Objaverse. This diverse dataset empowers our model to learn from a wide range of object variations, bolstering its ability to generate high-quality and diverse 3D shapes. Through extensive experimentation, we demonstrate the remarkable efficacy of our approach in significantly improving the visual quality of generated 3D shapes. By pushing the boundaries of 3D generation, introducing novel methods for latent representation learning, and harnessing the power of transformers for multi-modal conditional generation, our contributions pave the way for substantial advancements in the field. Our work unlocks new possibilities for applications in gaming, virtual reality, product design, and other domains that demand high-quality and diverse 3D objects.

1 Introduction

The field of 3D shape generation has gained significant attention due to its wide range of applications, and it continues to be an active area of research. Existing methods predominantly rely on generative adversarial networks (GANs) [76; 77; 1; 62; 6; 48; 5; 50; 24; 87; 53; 25; 75; 8; 39; 33; 28], variational autoencoders (VAEs) [46; 23; 22; 31], flows [81; 60; 30; 32], autoregressive models [68; 47; 27; 41], denoising diffusion probabilistic models (DDPMs) [82; 10; 73; 40; 86; 36; 63], and others. Despite recent advancements in 3D generative models, they still face significant challenges in meeting the requirements of real-world applications.

One major limitation of existing models is their inability to generate high-resolution 3D shapes with both quality and diversity. The resulting 3D shapes often suffer from low-level artifacts, lack of fine-grained textures, and insufficient details, which greatly impact their visual fidelity and realism. Additionally, these models exhibit a lack of diversity, often generating only a limited number of

---

[*]Equal contribution.
[†]Corresponding authors.

Preprint. Under review.

variations of similar shapes. This lack of diversity restricts their usability in applications that demand a broad range of high-quality 3D objects, such as gaming, virtual reality, and product design.

In our work, we draw inspiration from the remarkable achievements of large language models (LLMs) [70; 51; 54; 55; 3; 13; 85; 49; 71] and extend their success to the field of 3D generation. Specifically, we make significant contributions by adapting the Auto-Regressive model introduced in [42] and scaling it up to an unprecedented magnitude, named *Argus-3D*, comprising a remarkable 3.6 billion trainable parameters. This groundbreaking endeavor establishes our model as the largest 3D shape generation model known to date.

Our approach revolves around the acquisition of latent representations for 3D shapes, which we accomplish by training our model to learn tri-plane features, effectively reducing computational complexity. Additionally, we introduce a discrete codebook to effectively quantize these representations. Moreover, we employ transformers to predict the quantized representations, leveraging conditions to enable the generation of 3D shapes with multi-modal capabilities.

To facilitate the training of our expansive model, we harness the potential of an ensemble of publicly-available 3D datasets. Our training dataset comprises an impressive collection of nearly 800,000 objects sourced from prominent repositories such as ModelNet40 [79], ShapeNet [7], Pix3D [67], 3D-Future [21], and Objaverse [16]. Our experiments substantiate the efficacy of our approach, as our large-scale 3D generation model significantly enhances the visual quality of the generated 3D shapes.

Overall, our contributions lie in scaling 3D generation to unprecedented dimensions, developing a remarkable model with a vast number of parameters, exploring novel approaches for latent representation learning, introducing a discrete codebook for effective quantization, and leveraging transformers for multi-modal conditional generation. Through these advancements, we pave the way for substantial advancements in the field of 3D shape generation, enabling the generation of high-quality, diverse, and visually impressive 3D shapes.

2   Related work

3D Generative Models. Recently, there has been significant exploration of 3D shape generative models across various data formats, including polygen meshes[84; 41; 69], point clouds[57; 78; 2; 40], voxel grids[14; 43; 76; 34; 80], and implicit representations such as signed distance functions (SDFs)[9; 12; 45; 64; 52], among others. Each data format comes with its own advantages and disadvantages, making them suitable for different practical tasks. (1) Voxel representation inherits the ease of processing through 3D convolutions, similar to 2D images. However, it often suffers from low resolution due to its cubic space occupancy, with existing 3D generative models being limited to resolutions of 64^3 or lower. (2) Point clouds, extracted from shape surfaces, do not suffer from resolution restrictions and can handle a larger number of points. However, this representation lacks the ability to preserve 3D topological information and struggles with reconstructing detailed model surfaces. (3) Mesh-based methods represent 3D objects as a collection of vertices, edges, and faces, forming a polygonal mesh structure. This format is widely utilized due to its ability to represent complex geometry with relatively low storage requirements. However, memory consumption increases significantly as the number of polygons and vertices grows. (4) Implicit representations excel in representing high-resolution shapes with arbitrary topology. They can predict the signed distance function and recover shape surfaces through techniques like Marching Cubes. Despite the advancements in these different approaches, each has its own strengths and limitations. The choice of representation depends on the specific requirements of the application at hand.

Autoregressive Models. Autoregressive models are powerful probabilistic generative models that capture the distribution of probability density by factorizing the joint distribution into a series of conditional distributions using the probability chain rule. Unlike GANs, which lack a tractable probability density and often suffer from generation collisions, autoregressive models exhibit stability during training and have demonstrated their effectiveness in generating natural language, audio, and images[72; 56; 19]. However, in the context of 3D shape generation, most autoregressive models face challenges in producing high-quality shapes due to the lack of efficient representation. Recently, DDPMs[58; 26; 65; 17] have gained considerable attention for their stability and diverse image generation capabilities. DDPMs learn the data distribution from a Gaussian distribution through a gradual denoising process, often based on the U-Net[59] architecture. However, this approach
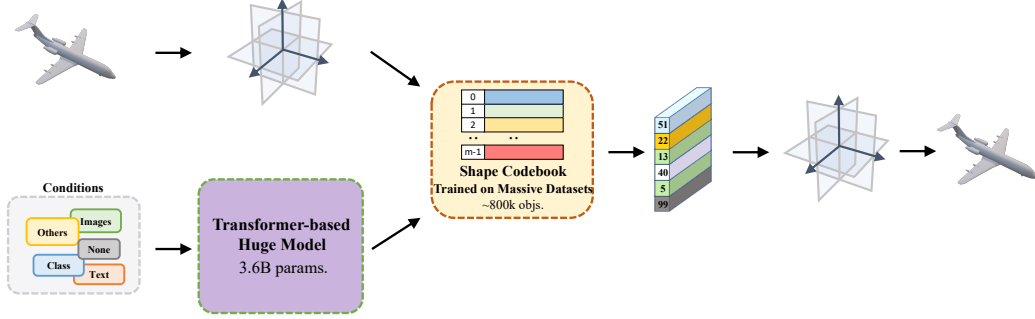
Figure 1: Overview of our model. We derive the shape features from arbitrary 3D shape via encoding points feature into the three normalized orthogonal planes, and project them into a latent vector. Next, a learnable codebook quantize it for discrete representation. These discrete representation assist the transformer in the second stage to learn the joint distribution corresponding to a large number of shape features encoded in the codebook. Futhermore, by concatenating various conditions such as images or text, transformer is capable of generate discrete representation for 3D shapes. We develop a remarkable 3D shape generalization model with 3.6 billion trainable parameters.

limits the resolution and extends the training cycles, thus hindering its performance in 3D generation. In contrast, transformer-based models offer a high degree of scalability, which has been shown to enhance performance across various downstream tasks by scaling up the model size[74; 49; 83; 15]. We posit that this scalability can also be advantageous in the domain of 3D shape generation, enabling more effective and efficient modeling of complex shapes.

3 Methodology

We adapt the Auto-Regressive model in [42] and scale up the learnable parameters. Our model is illustrated in Figure 1. We train the large model on a collection of 3D datasets. Training our 3D shape generation model consists of two stage. It first encodes the input into discrete representation and learns to decode the indices sequence of quantizer. Then, we train a transformer to generate the indices auto-regressively. So that the model is capable of generate high-quality and diverse 3D shapes.

3.1 Learning Discrete Representation

Firstly, we sample point clouds $\mathcal{P} \in \mathbb{R}^{n \times 3}$ from mesh as input, and utilize a PointNet[57] to obtain point features with dimension $\mathbb{R}^{n \times 32}$. These points are mapped to three axis-aligned orthogonal planes to obtain planar features $\mathbf{f}^v \in \mathbb{R}^{r \times r \times c \times 3}$, where r denote the resolution of feature plane amd c is the dimension. These features are then concatenated and projected to a serialized vector $\mathbf{z_v} \in \mathbb{R}^{(\bar{r} \times \bar{r}) \times d}$ using positional information, which allows us to maintain the order of the feature representations, where $\bar{r} = \frac{r}{8}$. Later, a learned discrete codebook $\mathbb{Z} = \{\mathbf{z}_k\}_{k=1}^K$ is used to quantize $\mathcal{Q}(\cdot)$:

$$\mathbf{z_q} = \mathcal{Q}(\mathbf{z}) := arg \min_{\mathbf{z}_k \in \mathbb{Z}} ||\mathbf{z}_i - \mathbf{z}_k||, \tag{1}$$

where $\mathbf{z}_i \subset \mathbb{R}^d$. We decode the tri-plane features from the quantized vector using a 2D U-Net. Last, we reconstruct voxel from plane feature and extracted the output shape with Marching Cubes[38].

By mapping 3D shape to three orthogonal planes, we can significantly reduce the computational complexity from being proportional to the cube resolution to being proportional to the square resolution, i.e. from $\mathcal{O}(r^3)$ to $\mathcal{O}(r^2)$, while still retaining the important spatial dependencies between points. To ensure that the representations retain the spatial dependencies between different points, we use convolutional neural networks (CNNs) to extract features from the planar representations, which are then concatenated and projected to a serialized vector with positional information to maintain the order of the feature representations. Different from [42], our model does not include the two fully connected layers between the quantized vectors and the encoder and decoder. We remove the two modules because the large model can learn to encode/decode the quantized vectors directly.

Optimization Objective. We optimize the parameters by minimizing the reconstruction error. We apply binary cross-entropy loss between the reconstruction occupancy values y_o and the input values y_i:

$$\mathcal{L}_{occ} = -(y_o \cdot log(y_i) + (1 - y_i) \cdot log(1 - y_o)) \tag{2}$$

The codebook loss, employed to minimize the discrepancy between the quantized representation and the feature vectors, is defined as follows:

$$\mathcal{L}_{quant} = ||sg[\mathbf{z_v}] - \mathbf{z_q}||_2^2 + \beta||sg[\mathbf{z_q}] - \mathbf{z_v}||_2^2 \tag{3}$$

Here, $sg[\cdot]$ denotes the stop-gratient operation, and $||sg[\mathbf{z_v}] - \mathbf{z_v}||_2^2$ is the *commitment loss* with weighting factor β, we set $\beta = 0.4$ by default. The overall reconstruction loss for the first stage is

$$\mathcal{L}_{rec} = \mathcal{L}_{occ} + \mathcal{L}_{quant} \tag{4}$$

3.2 Learning Shape Generation

We use a vinilla transformer to learn generate sequence indices of entries in the codebook. This indices represents discrete representation learning in first stage. Each input 3D shape has a tractable order and could be generate as a sequence indices. A learnable start-of-sequence token is used to predict the first index of the indices order. We feed discretized indices of latent vector $\mathbf{z} = \{\mathbf{z}_1, \mathbf{z}_2, \cdots, \mathbf{z}_m\}$ into transformer to learn retrieve the discrete indices. By learning the distribution of previous indices $p(\mathbf{z}_i|\mathbf{z}_{<i})$, the model can predict the next index with joint distribution:

$$p(\mathbf{z}) = \prod_{i=1}^{m} p(\mathbf{z}_i|\mathbf{z}_{<i}) \tag{5}$$

Joint Representation Learning By embedding condition information to a vector $\mathbf{c}$ and learn the joint distribution with transformer, our model can generation 3D shape in condition. In lieu of intricate module design or training strategies, we adopt a simpler approach by learning the joint distribution with given conditions $\mathbf{c}$, achieved by appending it to $\mathbf{z}$, As follow,

$$p(\mathbf{z}) = \prod_{i=1}^{m} p(\mathbf{z}_i|\mathbf{c}, \mathbf{z}_{<i}) \tag{6}$$

where $\mathbf{c}$ denotes a feature vector extracted from arbitrary forms of conditions *i.e.* one-dimensional text, audio, two-dimensional images, or three-dimensional point clouds *etc.*

Optimization Objective. To ensure that the generated data closely approximates the real distribution, we minimize the discrepancy between the generated samples and the real data distribution $p(\mathbf{x})$:

$$\mathcal{L}_{nll} = \mathbb{E}_{\mathbf{x} \sim p(\mathbf{x})}[-\log p(\mathbf{z})] \tag{7}$$

3.3 Scaling Up Model

Motivated by the remarkable progress observed in large language models, we embark on a transformative journey to scale up the 3D generation model, unearthing its untapped potential for substantial performance improvements. In our quest, we present noteworthy contributions by doubling the codebook number and dimension, elevating them to unprecedented heights at 8192 and 512, respectively, surpassing previous pioneering works. Drawing inspiration from the groundbreaking GPT3[4], we meticulously set the transformer layer, dimension, and head to 32, 3072, and 24, respectively. This deliberate orchestration culminates in the birth of an awe-inspiring 3D generation model, proudly boasting an astonishing 3.6 billion parameters. We denote it as *Ours-Huge*. We also derive a smaller version with 1.2 billion parameters for fast experiments, which is named *Ours-Large*. The only difference is that we set transformer layer, dimension, and head to be 24, 2048 and 16.

To the best of our knowledge, we highlight that our proposed model stands as the largest of its kind in the realm of 3D shape generation, eclipsing the parameter counts of renowned works such as SDFusion [11] and Shap-E [29], which consist of approximately 1 billion parameters. This monumental achievement in scaling up the model represents a significant milestone, propelling the field of 3D shape generation towards unparalleled advancements.

3.4 Scaling Up Data

In our quest to build a robust and diverse training dataset, we draw inspiration from the remarkable progress observed in the realm of 2D vision, where the effectiveness of large models fueled by ample training data has been extensively demonstrated [18; 35; 20]. However, we acknowledge the inherent challenges associated with constructing large-scale 3D shape datasets, as the process of labeling 3D objects entails considerably higher costs and complexities compared to their 2D counterparts.

In this paper, we proudly present our significant contributions, which revolve around the meticulous curation of a diverse and comprehensive collection of publicly-available 3D datasets. These datasets serve as invaluable resources for training and evaluation, enabling us to push the boundaries of 3D shape generation. Our curated dataset comprises:

ModelNet40[79]: This dataset stands as a valuable resource, containing an impressive collection of over 12,300 CAD models spanning 40 object categories. For our research objectives, we strategically select 9,843 models from this dataset to serve as the foundation for training our model. An additional 2,468 models are reserved for rigorous testing, enabling us to comprehensively evaluate the performance and generalization capabilities of our approach.

ShapeNet[7]: Recognized for its comprehensiveness and scope, ShapeNet provides an extensive and diverse collection of 3D models. Encompassing 55 common object categories and boasting over 51,300 unique 3D models, this dataset offers rich and varied representations that greatly enhance the training process of our model. The inclusion of ShapeNet in our dataset selection bolsters the ability of our model to capture a wide range of object variations and complexities.

Pix3D[67]: With its large-scale nature, Pix3D emerges as a valuable resource for our research. Comprising 10,069 images and 395 shapes, this dataset exhibits significant variations, allowing our model to learn from a diverse range of object appearances and characteristics. By incorporating Pix3D into our training dataset, we equip our model with the capability to generate visually impressive and realistic 3D shapes.

3D-Future[21]: As a specialized furniture dataset, 3D-Future provides a unique and detailed collection of 16,563 distinct 3D instances. By including this dataset in our training pipeline, we ensure that our model gains insights into the intricacies and nuances of furniture designs. This enables our model to generate high-quality and realistic 3D shapes in the furniture domain, facilitating its application in areas such as interior design and virtual staging.

Objaverse[16]: A recent addition to the realm of 3D shape datasets, Objaverse captivates us with its vastness and richness. Sourced from Sketchfab, this immensely large dataset comprises over 800,000(and growing) 3D models, offering a wide array of object categories and variations. This extensive dataset providing our model with a wealth of diverse and representative examples for learning and generating high-quality 3D shapes.

Through meticulous curation and the thoughtful incorporation of these prominent datasets, we ensure that our training process encapsulates a diverse and comprehensive spectrum of 3D object variations, laying the groundwork for remarkable advancements in the field of 3D shape generation.

In our endeavor, we amass an impressive collection comprising approximately 900,000 3D shapes. To prepare the data, we meticulously follow the established methodologies outlined in 3D-R2N2[14] and C-OccNet[44], employing techniques such as mesh-fusion[66] to create depth maps, generating watertight meshes, and sampling points from these meshes. It is worth noting that the generation of intermediate files from a single ShapeNet dataset can exceed 3TB during these intricate steps. For the Pix3D chair category, we leverage the provided train/test splits. Regarding the other datasets, we randomly select the 80% as training samples, while the remaining 20% is reserved for testing purposes. Due to the sheer size of the objaverse dataset, we selected only 10% of the dataset as the dedicated test set. All of these carefully curated datasets play a pivotal role in training our first-stage model, serving as the bedrock of our research endeavor.

4 Experiments

In our rigorous evaluation process, we employ the Intersection over Union (IoU) metric to assess the reconstruction performance of the first stage. Once the IoU surpasses the remarkable threshold of 0.9, a pivotal moment arrives, as we leverage the trained codebook to quantize the input data, ushering
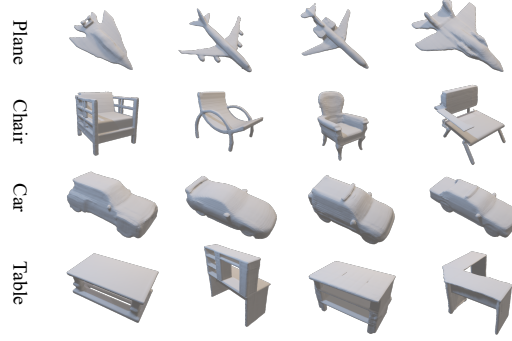
Figure 2: Qualitative results of unconditional generation.

forth the generation of corresponding index sequences. These meticulously quantized data then become the bedrock for training the autoregressive model of the second stage, fueling its remarkable capabilities.

To comprehensively gauge the prowess of our model, we embark on an extensive array of four distinctive experiments. Firstly, we delve into the realm of unconditional generation, showcasing our model's remarkable aptitude in crafting intricate shapes across four widely-used categories: planes, chairs, cars, and tables. Emboldened by this achievement, we venture further into the domain of conditional generation, where our model shines even brighter, effortlessly producing an array of faithful and diverse shapes across several intriguing tasks. The culmination of these experiments unveils the true potential of our model, positioning it at the forefront of cutting-edge 3D shape generation research.

4.1 Unconditional Generation

In the landscape of prior research[41; 45; 28], a prevailing approach involves training unconditional generation models on a per-category basis, subsequently evaluating their performance by generating samples exclusively from that specific category. This conventional framework, however, necessitates the training of separate models for each category, imposing substantial costs when working with large-scale models. Moreover, the relatively limited availability of data per category inherently constrains the potential and efficacy of our expansive models.

In light of these challenges, we adopt a pragmatic strategy, leveraging our insights to train multiple smaller models on commonly encountered categories. This judicious approach enables us to comprehensively assess the generative prowess of our models while circumventing the limitations imposed by category-specific training. The captivating results of our efforts are eloquently showcased in the accompanying Figure 2, where the rich diversity and remarkable fidelity of the generated samples beautifully exemplify the transformative capabilities of our approach.

4.2 Class-guide Generation

In our pursuit of enhancing the generative capabilities of our model, we undertake a comprehensive training approach that incorporates class conditioning across all 55 diverse categories from the ShapeNet dataset. This endeavor necessitates the availability of category labels to guide the shape generation process, facilitating the synthesis of shapes that align with the specific category characteristics.

Building upon the methodologies established by previous works [28; 9], we rigorously evaluate the performance of our model using a range of insightful metrics. The 1-Nearest Neighbor Accuracy (1-NNA) [37; 81] serves as our primary metric for measuring the distribution similarity, employing both the Chamfer distance (CD) and earth mover distance (EMD). Additionally, we utilize Coverage (COV) [2], Minimum Matching Distance (MMD) [2], and Edge Count Difference (ECD) [28] to assess the diversity, fidelity, and overall quality of the synthesized shapes.
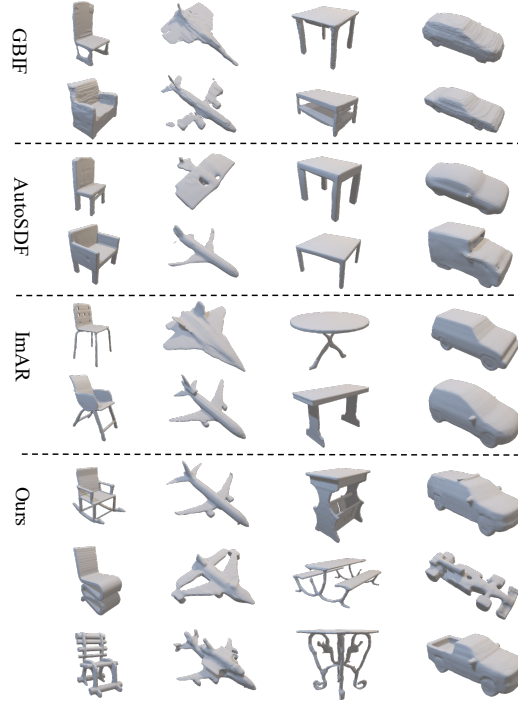
6

Figure 3: Qualitative results of class-guide generation.

To benchmark the performance of our model, we compare it against three baseline models, namely GBIF [28], AutoSDF [45], and ImAR [41]. As illustrated in Table 1, our huge model consistently outperforms the baselines across various metrics, signifying a substantial improvement in overall performance. It is worth noting that our model exhibits slightly lower performance in terms of MMD for the plane class. One possible explanation for this observation is that our model's encoding of 3D shapes to planar features may weaken the spatial constraints on flat objects, resulting in the generation of partially scattered points.

We visualize generated shapes with multiple categories in Figure 3.

Our generated shapes are characterized by intricate details and complex structures, which also significantly contribute to the diversity of the results. To fully appreciate the effect, please zoom in and observe the fine-grained intricacies.

4.3 Image-guide Generation

Undertaking the task of image-guided generation presents a greater challenge, necessitating the utilization of a pretrained CLIP model to extract 2D feature vectors from images, which serve as conditions for our model.

To generate quantized sequences, we make use of all the datasets from the training set of the first stage, excluding ModelNet. These quantized sequences are then paired with randomly rendered multi-view images, resulting in single-view image-shape pairs that serve as training data.

Following the established approach in previous works, we evaluate our models by randomly sampling 50 single-view images from the test split of 13 categories. For each image, we generate 5 shapes for evaluation purposes. To assess the diversity, we employ the Total Mutual Difference (TMD) metric, while the faithfulness of completed shapes is measured using MMD.

Table 2 show our large model achieves state-of-the-art performance on image-guide shape generation. It is worth noting that our image-guided model not only achieves higher fidelity than previous state-of-the-art methods but also significantly boosts diversity in performance. Qualitative results of our image-guided generation approach are presented in Figure 4.

7

Category	Model	MMD($\times 10^3$)↓		COV(%)↑		1-NNA(%)↓		ECD↓	
		CD	EMD	CD	EMD	CD	EMD	CD	EMD
Plane	GBIF [28]	1.4394	1.1348	42.33	45.30	89.23	79.83	1563	1355
	AutoSDF [45]	4.8047	2.4814	26.57	31.32	80.66	79.30	4750	5101
	ImAR [41]	**1.0577**	**0.8587**	49.01	50.99	63.49	55.32	43	92
	Ours	1.0998	0.8680	**50.25**	**56.68**	**58.66**	**48.89**	**2**	**58**
Chair	GBIF [28]	4.2520	2.3369	49.63	52.73	68.46	62.85	184	290
	AutoSDF [45]	5.5206	2.7157	34.71	37.67	81.39	76.29	3166	2991
	ImAR [41]	4.1144	2.2620	49.63	51.85	59.90	56.94	79	183
	Ours	**3.7802**	**2.1334**	**51.55**	**53.62**	**54.51**	**52.36**	**6**	**95**
Table	GBIF [28]	3.4813	2.1010	50.89	53.86	66.67	62.99	98	457
	AutoSDF [45]	4.8047	2.4814	26.57	31.32	80.66	79.30	4750	5101
	ImAR [41]	3.3972	1.9795	48.64	53.86	56.17	53.68	52	114
	Ours	**3.0622**	**1.8813**	**54.45**	**54.21**	**50.83**	**50.18**	**1**	**87**
Car	GBIF [28]	1.2853	0.9062	33.71	40.00	90.00	79.14	2453	1471
	AutoSDF [45]	1.2695	0.8739	34.86	41.71	88.29	80.71	2312	1299
	ImAR [41]	1.1929	0.8704	36.45	37.38	73.77	72.43	1823	2231
	Ours	**1.0901**	**0.8104**	**40.57**	**42.00**	**72.14**	**65.14**	**472**	**430**
Avg	GBIF [28]	2.6145	1.6197	44.14	47.97	78.59	71.20	1075	894
	AutoSDF [45]	3.3977	1.9046	28.62	32.94	84.93	81.48	3669	3535
	ImAR [41]	2.4406	1.4927	45.93	48.52	63.33	59.59	500	656
	Ours	**2.2581**	**1.4232**	**49.21**	**51.63**	**59.04**	**54.15**	**120**	**168**

Table 1: Results of class-guide generation. Models are trained on 55 categories of ShapeNet and generate shapes with categories label.
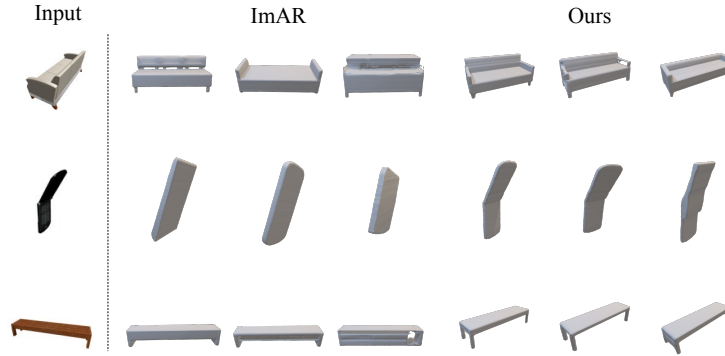

Figure 4: Visualizations of image-guide shape generation.

Additionally, we explore the generalizability of our model on real-world images. By conditioning our model on Pix3D images, we demonstrate its ability to accurately capture the primary attributes of objects depicted in the images, generating highly quality associated 3D shapes. The remarkable results of this investigation are showcased in the accompanying Figure5.

4.4 Text-guide Generation

By harnessing the remarkable bridging capabilities of the CLIP model between text and image modalities, our model transcends the boundaries of traditional input sources and enables the generation of 3D shapes solely from zero-shot textual input. During the training phase, we adhered to the methodology outlined in 4.3, utilizing paired image-shape inputs. However, during the inference stage, we took a groundbreaking approach by substituting the image features with text features extracted from CLIP.

Figure 5: Results of real-world image-guide generation.

Method	TMD ($\times 10^2$) ↑	MMD ($\times 10^3$) ↓	FPD ↓
AutoSDF [45]	2.657	2.137	15.262
CLIP-Forge [61]	2.858	1.926	8.094
ImAR [41]	4.274	1.590	1.680
Ours-Large	**7.343**	**1.523**	**1.467**

Table 2: Quantitative results of image-guide generation.

The accompanying figure serves as a visual testament to the impressive generative prowess of our model, showcasing the diverse and captivating 3D shape outputs generated in response to different textual prompts. This groundbreaking advancement exemplifies the power and versatility of our model, as it seamlessly operates across multiple input modalities, opening up exciting new avenues in the realm of 3D shape generation. As shown in Figure 6, our model excels at generating fine-grained shapes, surpassing previous zero-shot approaches. Additionally, we showcase the diversity of our text-guided shape generation through Figure 7

5   Ablation Study

In order to investigate the impact of increasing model parameters on performance, we followed the parameter configuration of GPT-3 and trained three models of different sizes: Small(100M), Large(1.2B), and Huge(3.6B), both based on first stage shape codebook with 8192 entries, 512 dimensions. Table 3 illustrates the parameter comparison among our different models.
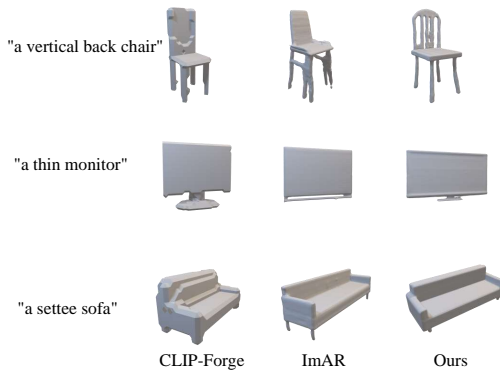

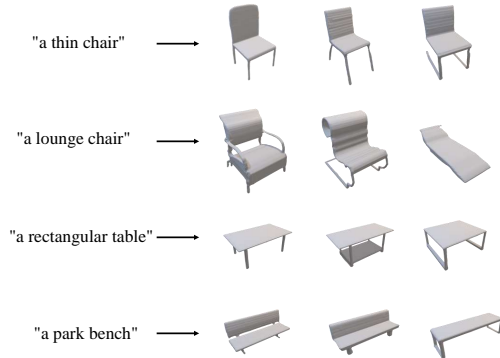Figure 6: Qualitative comparisons with the previous zero-shot methods.

Figure 7: Results of zero-shot text-to-shape generation.

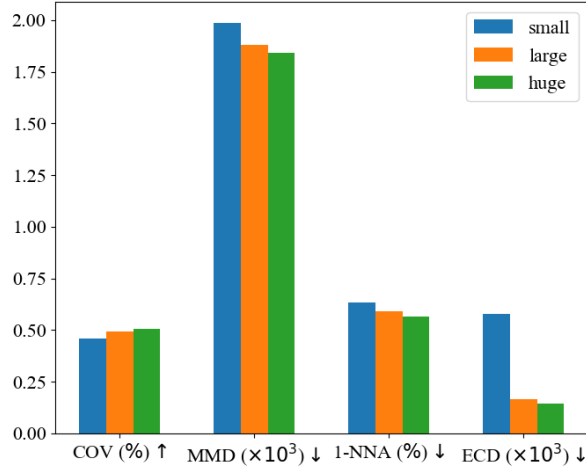| Size	Dimensions	Layers	Heads	Params [M]
Small	768	12	12	100
Large	2048	24	16	1239
Huge	3072	32	24	3670

Table 3: Model architecture details.

Figure 8: Quantitative result for different models.

We evaluated the different models on class-guide generation task. As show in Figure 8, our huge model achieved better performance across multiple metrics. Especially in terms of ECD indicators, larger models have shown significant improvement compared to smaller models.

Validation of Generative Capacity   In order to further demonstrate that our huge model has learned the underlying distribution of the 3D shape rather than simply memorizing the training set to reconstruct shape, we selected the generated samples and calculated their nearest neighbors in the training set based on Chamfer Distance. Figure 9 show our results.
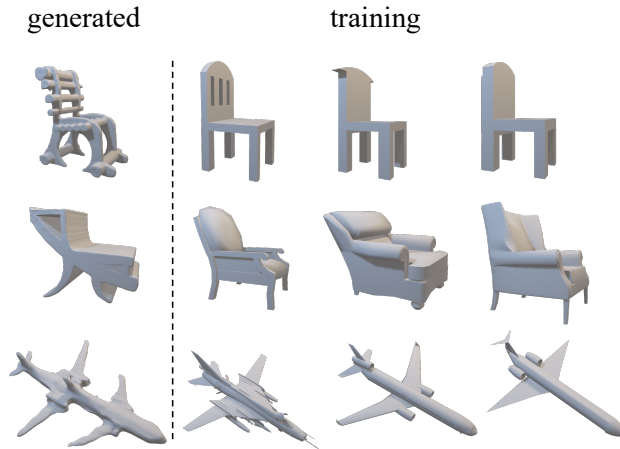

Figure 9: Generated novel shapes with similar shapes retrieval. We look up the top-3 nearest neighbor from the training set based on Chamfer Distance.

6 Conclusion

In this paper, we explore the limits of 3D shape generation by scaling the adapted Auto-Regressive model to 3.6 billion parameters and train it on the collected dataset with approximately 900,000 objects. Our larger-scale dataset and increased model parameters enable us to generate a wider variety and complexity of spatial structures, particularly intricate objects like chairs. The comprehensive dataset captures diverse designs and styles, allowing our model to learn underlying patterns effectively.

However, challenges remain, including the need for ample training data and the computational demands of the transformer architecture. To address these, we're exploring domain-specific knowledge integration, more efficient transformer architectures, and novel 3D shape data representations. These efforts aim to enhance our approach's performance and overcome existing challenges.

References

[1] Rameen Abdal, Hsin-Ying Lee, Peihao Zhu, Menglei Chai, Aliaksandr Siarohin, Peter Wonka, and Sergey Tulyakov. 3davatargan: Bridging domains for personalized editable avatars. *arXiv preprint arXiv:2301.02700*, 2023.

[2] Panos Achlioptas, Olga Diamanti, Ioannis Mitliagkas, and Leonidas Guibas. Learning representations and generative models for 3d point clouds. In *International conference on machine learning*, pages 40–49. PMLR, 2018.

[3] Tom Brown, Benjamin Mann, Nick Ryder, Melanie Subbiah, Jared D Kaplan, Prafulla Dhariwal, Arvind Neelakantan, Pranav Shyam, Girish Sastry, Amanda Askell, et al. Language models are few-shot learners. *Advances in neural information processing systems*, 33:1877–1901, 2020.

[4] Tom Brown, Benjamin Mann, Nick Ryder, Melanie Subbiah, Jared D Kaplan, Prafulla Dhariwal, Arvind Neelakantan, Pranav Shyam, Girish Sastry, Amanda Askell, et al. Language models are few-shot learners. *Advances in neural information processing systems*, 33:1877–1901, 2020.

[5] Eric R Chan, Connor Z Lin, Matthew A Chan, Koki Nagano, Boxiao Pan, Shalini De Mello, Orazio Gallo, Leonidas J Guibas, Jonathan Tremblay, Sameh Khamis, et al. Efficient geometry-aware 3d generative adversarial networks. In *Proceedings of the IEEE/CVF Conference on Computer Vision and Pattern Recognition*, pages 16123–16133, 2022.

[6] Eric R Chan, Marco Monteiro, Petr Kellnhofer, Jiajun Wu, and Gordon Wetzstein. pi-gan: Periodic implicit generative adversarial networks for 3d-aware image synthesis. In *Proceedings of the IEEE/CVF conference on computer vision and pattern recognition*, pages 5799–5809, 2021.

[7] Angel X Chang, Thomas Funkhouser, Leonidas Guibas, Pat Hanrahan, Qixing Huang, Zimo Li, Silvio Savarese, Manolis Savva, Shuran Song, Hao Su, et al. Shapenet: An information-rich 3d model repository. *arXiv preprint arXiv:1512.03012*, 2015.

[8] Zhiqin Chen, Vladimir G Kim, Matthew Fisher, Noam Aigerman, Hao Zhang, and Siddhartha Chaudhuri. Decor-gan: 3d shape detailization by conditional refinement. In *Proceedings of the IEEE/CVF conference on computer vision and pattern recognition*, pages 15740–15749, 2021.

[9] Zhiqin Chen and Hao Zhang. Learning implicit fields for generative shape modeling. In *Proceedings of the IEEE/CVF Conference on Computer Vision and Pattern Recognition*, pages 5939–5948, 2019.

[10] Yen-Chi Cheng, Hsin-Ying Lee, Sergey Tulyakov, Alexander Schwing, and Liangyan Gui. Sdfusion: Multimodal 3d shape completion, reconstruction, and generation. *arXiv preprint arXiv:2212.04493*, 2022.

[11] Yen-Chi Cheng, Hsin-Ying Lee, Sergey Tuyakov, Alex Schwing, and Liangyan Gui. SDFusion: Multimodal 3d shape completion, reconstruction, and generation. In *CVPR*, 2023.

[12] Zezhou Cheng, Menglei Chai, Jian Ren, Hsin-Ying Lee, Kyle Olszewski, Zeng Huang, Subhransu Maji, and Sergey Tulyakov. Cross-modal 3d shape generation and manipulation. In *Computer Vision–ECCV 2022: 17th European Conference, Tel Aviv, Israel, October 23–27, 2022, Proceedings, Part III*, pages 303–321. Springer, 2022.

[13] Aakanksha Chowdhery, Sharan Narang, Jacob Devlin, Maarten Bosma, Gaurav Mishra, Adam Roberts, Paul Barham, Hyung Won Chung, Charles Sutton, Sebastian Gehrmann, et al. Palm: Scaling language modeling with pathways. *arXiv preprint arXiv:2204.02311*, 2022.

[14] Christopher B Choy, Danfei Xu, JunYoung Gwak, Kevin Chen, and Silvio Savarese. 3d-r2n2: A unified approach for single and multi-view 3d object reconstruction. In *Computer Vision–ECCV 2016: 14th European Conference, Amsterdam, The Netherlands, October 11-14, 2016, Proceedings, Part VIII 14*, pages 628–644. Springer, 2016.

[15] Mostafa Dehghani, Josip Djolonga, Basil Mustafa, Piotr Padlewski, Jonathan Heek, Justin Gilmer, Andreas Steiner, Mathilde Caron, Robert Geirhos, Ibrahim Alabdulmohsin, et al. Scaling vision transformers to 22 billion parameters. *arXiv preprint arXiv:2302.05442*, 2023.

[16] Matt Deitke, Dustin Schwenk, Jordi Salvador, Luca Weihs, Oscar Michel, Eli VanderBilt, Ludwig Schmidt, Kiana Ehsani, Aniruddha Kembhavi, and Ali Farhadi. Objaverse: A universe of annotated 3d objects. *arXiv preprint arXiv:2212.08051*, 2022.

[17] Prafulla Dhariwal and Alexander Nichol. Diffusion models beat gans on image synthesis. *Advances in Neural Information Processing Systems*, 34:8780–8794, 2021.

[18] Alexey Dosovitskiy, Lucas Beyer, Alexander Kolesnikov, Dirk Weissenborn, Xiaohua Zhai, Thomas Unterthiner, Mostafa Dehghani, Matthias Minderer, Georg Heigold, Sylvain Gelly, et al. An image is worth 16x16 words: Transformers for image recognition at scale. *International Conference on Learning Representations (ICLR)*, 2021.

[19] Patrick Esser, Robin Rombach, and Bjorn Ommer. Taming transformers for high-resolution image synthesis. In *Proceedings of the IEEE/CVF conference on computer vision and pattern recognition*, pages 12873–12883, 2021.

[20] Yuxin Fang, Wen Wang, Binhui Xie, Quan Sun, Ledell Wu, Xinggang Wang, Tiejun Huang, Xinlong Wang, and Yue Cao. Eva: Exploring the limits of masked visual representation learning at scale. *arXiv preprint arXiv:2211.07636*, 2022.

[21] Huan Fu, Rongfei Jia, Lin Gao, Mingming Gong, Binqiang Zhao, Steve Maybank, and Dacheng Tao. 3d-future: 3d furniture shape with texture. *International Journal of Computer Vision*, 129:3313–3337, 2021.

[22] Lin Gao, Tong Wu, Yu-Jie Yuan, Ming-Xian Lin, Yu-Kun Lai, and Hao Zhang. Tm-net: Deep generative networks for textured meshes. *ACM Transactions on Graphics (TOG)*, 40(6):1–15, 2021.

[23] Lin Gao, Jie Yang, Tong Wu, Yu-Jie Yuan, Hongbo Fu, Yu-Kun Lai, and Hao Zhang. Sdm-net: Deep generative network for structured deformable mesh. *ACM Transactions on Graphics (TOG)*, 38(6):1–15, 2019.

[24] Jiatao Gu, Lingjie Liu, Peng Wang, and Christian Theobalt. Stylenerf: A style-based 3d-aware generator for high-resolution image synthesis, 2021.

[25] Zekun Hao, Arun Mallya, Serge Belongie, and Ming-Yu Liu. Gancraft: Unsupervised 3d neural rendering of minecraft worlds. In *Proceedings of the IEEE/CVF International Conference on Computer Vision*, pages 14072–14082, 2021.

[26] Jonathan Ho, Ajay Jain, and Pieter Abbeel. Denoising diffusion probabilistic models, 2020.

[27] Moritz Ibing, Gregor Kobsik, and Leif Kobbelt. Octree transformer: Autoregressive 3d shape generation on hierarchically structured sequences. *arXiv preprint arXiv:2111.12480*, 2021.

[28] Moritz Ibing, Isaak Lim, and Leif Kobbelt. 3d shape generation with grid-based implicit functions. In *Proceedings of the IEEE/CVF Conference on Computer Vision and Pattern Recognition*, pages 13559–13568, 2021.

[29] Heewoo Jun and Alex Nichol. Shap-e: Generating conditional 3d implicit functions. *arXiv preprint arXiv:2305.02463*, 2023.

[30] Hyeongju Kim, Hyeonseung Lee, Woo Hyun Kang, Joun Yeop Lee, and Nam Soo Kim. Softflow: Probabilistic framework for normalizing flow on manifolds. *Advances in Neural Information Processing Systems*, 33:16388–16397, 2020.

[31] Jinwoo Kim, Jaehoon Yoo, Juho Lee, and Seunghoon Hong. Setvae: Learning hierarchical composition for generative modeling of set-structured data. In *Proceedings of the IEEE/CVF Conference on Computer Vision and Pattern Recognition*, pages 15059–15068, 2021.

[32] Roman Klokov, Edmond Boyer, and Jakob Verbeek. Discrete point flow networks for efficient point cloud generation. In *Computer Vision–ECCV 2020: 16th European Conference, Glasgow, UK, August 23–28, 2020, Proceedings, Part XXIII 16*, pages 694–710. Springer, 2020.

[33] Ruihui Li, Xianzhi Li, Ka-Hei Hui, and Chi-Wing Fu. Sp-gan: Sphere-guided 3d shape generation and manipulation. *ACM Transactions on Graphics (TOG)*, 40(4):1–12, 2021.

[34] Chieh Hubert Lin, Hsin-Ying Lee, Willi Menapace, Menglei Chai, Aliaksandr Siarohin, Ming-Hsuan Yang, and Sergey Tulyakov. Infinicity: Infinite-scale city synthesis. *arXiv preprint arXiv:2301.09637*, 2023.

[35] Ze Liu, Yutong Lin, Yue Cao, Han Hu, Yixuan Wei, Zheng Zhang, Stephen Lin, and Baining Guo. Swin transformer: Hierarchical vision transformer using shifted windows. In *Proceedings of the IEEE/CVF international conference on computer vision*, pages 10012–10022, 2021.

[36] Zhen Liu, Yao Feng, Michael J Black, Derek Nowrouzezahrai, Liam Paull, and Weiyang Liu. Meshdiffusion: Score-based generative 3d mesh modeling. *arXiv preprint arXiv:2303.08133*, 2023.

[37] David Lopez-Paz and Maxime Oquab. Revisiting classifier two-sample tests. *arXiv preprint arXiv:1610.06545*, 2016.

[38] William E Lorensen and Harvey E Cline. Marching cubes: A high resolution 3d surface construction algorithm. *ACM siggraph computer graphics*, 21(4):163–169, 1987.

[39] Andrew Luo, Tianqin Li, Wen-Hao Zhang, and Tai Sing Lee. Surfgen: Adversarial 3d shape synthesis with explicit surface discriminators. In *Proceedings of the IEEE/CVF International Conference on Computer Vision*, pages 16238–16248, 2021.

[40] Shitong Luo and Wei Hu. Diffusion probabilistic models for 3d point cloud generation. In *Proceedings of the IEEE/CVF Conference on Computer Vision and Pattern Recognition*, pages 2837–2845, 2021.

[41] Simian Luo, Xuelin Qian, Yanwei Fu, Yinda Zhang, Ying Tai, Zhenyu Zhang, Chengjie Wang, and Xiangyang Xue. Learning versatile 3d shape generation with improved ar models. *arXiv preprint arXiv:2303.14700*, 2023.

[42] Simian Luo, Xuelin Qian, Yanwei Fu, Yinda Zhang, Ying Tai, Zhenyu Zhang, Chengjie Wang, and Xiangyang Xue. Learning versatile 3d shape generation with improved ar models. *arXiv preprint arXiv:2303.14700*, 2023.

[43] Daniel Maturana and Sebastian Scherer. Voxnet: A 3d convolutional neural network for real-time object recognition. In *2015 IEEE/RSJ international conference on intelligent robots and systems (IROS)*, pages 922–928. IEEE, 2015.

[44] Lars Mescheder, Michael Oechsle, Michael Niemeyer, Sebastian Nowozin, and Andreas Geiger. Occupancy networks: Learning 3d reconstruction in function space. In *Proceedings of the IEEE/CVF conference on computer vision and pattern recognition*, pages 4460–4470, 2019.

[45] Paritosh Mittal, Yen-Chi Cheng, Maneesh Singh, and Shubham Tulsiani. Autosdf: Shape priors for 3d completion, reconstruction and generation. In *Proceedings of the IEEE/CVF Conference on Computer Vision and Pattern Recognition*, pages 306–315, 2022.

[46] Kaichun Mo, Paul Guerrero, Li Yi, Hao Su, Peter Wonka, Niloy Mitra, and Leonidas J Guibas. Structurenet: Hierarchical graph networks for 3d shape generation. *arXiv preprint arXiv:1908.00575*, 2019.

[47] Charlie Nash, Yaroslav Ganin, SM Ali Eslami, and Peter Battaglia. Polygen: An autoregressive generative model of 3d meshes. In *International conference on machine learning*, pages 7220–7229. PMLR, 2020.

[48] Michael Niemeyer and Andreas Geiger. Giraffe: Representing scenes as compositional generative neural feature fields. In *Proceedings of the IEEE/CVF Conference on Computer Vision and Pattern Recognition*, pages 11453–11464, 2021.

[49] OpenAI. Gpt-4 technical report, 2023.

[50] Roy Or-El, Xuan Luo, Mengyi Shan, Eli Shechtman, Jeong Joon Park, and Ira Kemelmacher-Shlizerman. Stylesdf: High-resolution 3d-consistent image and geometry generation. In *Proceedings of the IEEE/CVF Conference on Computer Vision and Pattern Recognition*, pages 13503–13513, 2022.

[51] Long Ouyang, Jeffrey Wu, Xu Jiang, Diogo Almeida, Carroll Wainwright, Pamela Mishkin, Chong Zhang, Sandhini Agarwal, Katarina Slama, Alex Ray, et al. Training language models to follow instructions with human feedback. *Advances in Neural Information Processing Systems*, 35:27730–27744, 2022.

[52] Jeong Joon Park, Peter Florence, Julian Straub, Richard Newcombe, and Steven Lovegrove. Deepsdf: Learning continuous signed distance functions for shape representation. In *Proceedings of the IEEE/CVF conference on computer vision and pattern recognition*, pages 165–174, 2019.

[53] Dario Pavllo, Jonas Kohler, Thomas Hofmann, and Aurelien Lucchi. Learning generative models of textured 3d meshes from real-world images. In *Proceedings of the IEEE/CVF International Conference on Computer Vision*, pages 13879–13889, 2021.

[54] Alec Radford, Karthik Narasimhan, Tim Salimans, Ilya Sutskever, et al. Improving language understanding by generative pre-training. 2018.

[55] Alec Radford, Jeffrey Wu, Rewon Child, David Luan, Dario Amodei, Ilya Sutskever, et al. Language models are unsupervised multitask learners. *OpenAI blog*, 1(8):9, 2019.

[56] Ali Razavi, Aaron Van den Oord, and Oriol Vinyals. Generating diverse high-fidelity images with vq-vae-2. *Advances in neural information processing systems*, 32, 2019.

[57] Gernot Riegler, Ali Osman Ulusoy, Horst Bischof, and Andreas Geiger. Octnetfusion: Learning depth fusion from data. In *2017 International Conference on 3D Vision (3DV)*, pages 57–66. IEEE, 2017.

[58] Robin Rombach, Andreas Blattmann, Dominik Lorenz, Patrick Esser, and Björn Ommer. High-resolution image synthesis with latent diffusion models. In *Proceedings of the IEEE/CVF Conference on Computer Vision and Pattern Recognition*, pages 10684–10695, 2022.

[59] Olaf Ronneberger, Philipp Fischer, and Thomas Brox. U-net: Convolutional networks for biomedical image segmentation, 2015.

[60] Aditya Sanghi, Hang Chu, Joseph G Lambourne, Ye Wang, Chin-Yi Cheng, Marco Fumero, and Kamal Rahimi Malekshan. Clip-forge: Towards zero-shot text-to-shape generation. In *Proceedings of the IEEE/CVF Conference on Computer Vision and Pattern Recognition*, pages 18603–18613, 2022.

[61] Aditya Sanghi, Hang Chu, Joseph G Lambourne, Ye Wang, Chin-Yi Cheng, Marco Fumero, and Kamal Rahimi Malekshan. Clip-forge: Towards zero-shot text-to-shape generation. In *Proceedings of the IEEE/CVF Conference on Computer Vision and Pattern Recognition*, pages 18603–18613, 2022.

[62] Katja Schwarz, Yiyi Liao, Michael Niemeyer, and Andreas Geiger. Graf: Generative radiance fields for 3d-aware image synthesis. *Advances in Neural Information Processing Systems*, 33:20154–20166, 2020.

[63] Jaehyeok Shim, Changwoo Kang, and Kyungdon Joo. Diffusion-based signed distance fields for 3d shape generation. In *Proceedings of the IEEE/CVF Conference on Computer Vision and Pattern Recognition*, pages 20887–20897, 2023.

[64] Vincent Sitzmann, Eric Chan, Richard Tucker, Noah Snavely, and Gordon Wetzstein. Metasdf: Meta-learning signed distance functions. *Advances in Neural Information Processing Systems*, 33:10136–10147, 2020.

[65] Jiaming Song, Chenlin Meng, and Stefano Ermon. Denoising diffusion implicit models. *arXiv preprint arXiv:2010.02502*, 2020.

[66] David Stutz and Andreas Geiger. Learning 3d shape completion under weak supervision. *CoRR*, abs/1805.07290, 2018.

[67] Xingyuan Sun, Jiajun Wu, Xiuming Zhang, Zhoutong Zhang, Chengkai Zhang, Tianfan Xue, Joshua B Tenenbaum, and William T Freeman. Pix3d: Dataset and methods for single-image 3d shape modeling. In *Proceedings of the IEEE conference on computer vision and pattern recognition*, pages 2974–2983, 2018.

[68] Yongbin Sun, Yue Wang, Ziwei Liu, Joshua Siegel, and Sanjay Sarma. Pointgrow: Autoregressively learned point cloud generation with self-attention. In *Proceedings of the IEEE/CVF Winter Conference on Applications of Computer Vision*, pages 61–70, 2020.

[69] Qingyang Tan, Lin Gao, Yu-Kun Lai, and Shihong Xia. Variational autoencoders for deforming 3d mesh models. In *Proceedings of the IEEE conference on computer vision and pattern recognition*, pages 5841–5850, 2018.

[70] Romal Thoppilan, Daniel De Freitas, Jamie Hall, Noam Shazeer, Apoorv Kulshreshtha, Heng-Tze Cheng, Alicia Jin, Taylor Bos, Leslie Baker, Yu Du, et al. Lamda: Language models for dialog applications. *arXiv preprint arXiv:2201.08239*, 2022.

[71] Hugo Touvron, Thibaut Lavril, Gautier Izacard, Xavier Martinet, Marie-Anne Lachaux, Timothée Lacroix, Baptiste Rozière, Naman Goyal, Eric Hambro, Faisal Azhar, Aurelien Rodriguez, Armand Joulin, Edouard Grave, and Guillaume Lample. Llama: Open and efficient foundation language models, 2023.

[72] Aaron Van den Oord, Nal Kalchbrenner, Lasse Espeholt, Oriol Vinyals, Alex Graves, et al. Conditional image generation with pixelcnn decoders. *Advances in neural information processing systems*, 29, 2016.

[73] Tengfei Wang, Bo Zhang, Ting Zhang, Shuyang Gu, Jianmin Bao, Tadas Baltrusaitis, Jingjing Shen, Dong Chen, Fang Wen, Qifeng Chen, et al. Rodin: A generative model for sculpting 3d digital avatars using diffusion. *arXiv preprint arXiv:2212.06135*, 2022.

[74] Jason Wei, Yi Tay, Rishi Bommasani, Colin Raffel, Barret Zoph, Sebastian Borgeaud, Dani Yogatama, Maarten Bosma, Denny Zhou, Donald Metzler, et al. Emergent abilities of large language models. *arXiv preprint arXiv:2206.07682*, 2022.

[75] Cheng Wen, Baosheng Yu, and Dacheng Tao. Learning progressive point embeddings for 3d point cloud generation. In *Proceedings of the IEEE/CVF Conference on Computer Vision and Pattern Recognition*, pages 10266–10275, 2021.

[76] Jiajun Wu, Chengkai Zhang, Tianfan Xue, Bill Freeman, and Josh Tenenbaum. Learning a probabilistic latent space of object shapes via 3d generative-adversarial modeling. *Advances in neural information processing systems*, 29, 2016.

[77] Rundi Wu, Xuelin Chen, Yixin Zhuang, and Baoquan Chen. Multimodal shape completion via conditional generative adversarial networks. In *Computer Vision–ECCV 2020: 16th European Conference, Glasgow, UK, August 23–28, 2020, Proceedings, Part IV 16*, pages 281–296. Springer, 2020.

[78] Wenxuan Wu, Zhongang Qi, and Li Fuxin. Pointconv: Deep convolutional networks on 3d point clouds. In *Proceedings of the IEEE/CVF Conference on computer vision and pattern recognition*, pages 9621–9630, 2019.

[79] Zhirong Wu, Shuran Song, Aditya Khosla, Fisher Yu, Linguang Zhang, Xiaoou Tang, and Jianxiong Xiao. 3d shapenets: A deep representation for volumetric shapes. In *Proceedings of the IEEE conference on computer vision and pattern recognition*, pages 1912–1920, 2015.

[80] Jianwen Xie, Zilong Zheng, Ruiqi Gao, Wenguan Wang, Song-Chun Zhu, and Ying Nian Wu. Learning descriptor networks for 3d shape synthesis and analysis. In *Proceedings of the IEEE conference on computer vision and pattern recognition*, pages 8629–8638, 2018.

[81] Guandao Yang, Xun Huang, Zekun Hao, Ming-Yu Liu, Serge Belongie, and Bharath Hariharan. Pointflow: 3d point cloud generation with continuous normalizing flows. In *Proceedings of the IEEE/CVF international conference on computer vision*, pages 4541–4550, 2019.

[82] Xiaohui Zeng, Arash Vahdat, Francis Williams, Zan Gojcic, Or Litany, Sanja Fidler, and Karsten Kreis. Lion: Latent point diffusion models for 3d shape generation. *arXiv preprint arXiv:2210.06978*, 2022.

[83] Xiaohua Zhai, Alexander Kolesnikov, Neil Houlsby, and Lucas Beyer. Scaling vision transformers. In *Proceedings of the IEEE/CVF Conference on Computer Vision and Pattern Recognition*, pages 12104–12113, 2022.

[84] Song-Hai Zhang, Yuan-Chen Guo, and Qing-Wen Gu. Sketch2model: View-aware 3d modeling from single free-hand sketches. In *Proceedings of the IEEE/CVF Conference on Computer Vision and Pattern Recognition*, pages 6012–6021, 2021.

[85] Susan Zhang, Stephen Roller, Naman Goyal, Mikel Artetxe, Moya Chen, Shuohui Chen, Christopher Dewan, Mona Diab, Xian Li, Xi Victoria Lin, et al. Opt: Open pre-trained transformer language models. *arXiv preprint arXiv:2205.01068*, 2022.

[86] Linqi Zhou, Yilun Du, and Jiajun Wu. 3d shape generation and completion through point-voxel diffusion. In *Proceedings of the IEEE/CVF International Conference on Computer Vision*, pages 5826–5835, 2021.

[87] Peng Zhou, Lingxi Xie, Bingbing Ni, and Qi Tian. Cips-3d: A 3d-aware generator of gans based on conditionally-independent pixel synthesis. *arXiv preprint arXiv:2110.09788*, 2021.